Gas-Phase Hydroxyl Radical Emission in the Thermal Decomposition of Lithium Hydroxide

Suguru Noda,* Masateru Nishioka, and Masayoshi Sadakata

Department of Chemical System Engineering, Graduate School of Engineering, The University of Tokyo, 7-3-1, Hongo, Bunkyo-ku, Tokyo 113-8656, Japan

Received: October 23, 1998; In Final Form: January 4, 1999

The gas-phase hydroxyl (OH) radical emission was observed in the thermal decomposition of lithium hydroxide (LiOH). This phenomenon was investigated in a vacuum flow tube reactor at around 2 Torr by the temperature programmed reaction (TPR) experiments at 500−1300 K. The production of OH and other gaseous products was quantitatively investigated by the laser induced fluorescence method and quadrupole mass spectrometry, respectively. The TPR spectra of OH had a peak at 1100−1200 K, which largely exceeded the gas-phase thermodynamic equilibrium. The origin of OH was supposed to be either the surface OH groups on Li_2O or the residual LiOH in the LiOH/Li_2O solid solution. OH production exceeding the thermodynamic equilibrium was explained by means of the partial equilibrium in the reaction: $LiOH + {}^1/_4O_2 \leftrightarrow {}^1/_2Li_2O + OH$. This phenomenon can be a new route for the OH production from H_2O and O_2 in cyclic reactions of lithium compounds.

Introduction

Gas-phase hydroxyl (OH) radicals are strong oxidizing agents and known to be important chain carriers in combustion and in atmospheric chemistry,[1] so they are expected to act as promoters in some reactions such as the catalytic combustion.[2] As for the OH production in the gas−solid interface, the heterogeneous catalytic reactions were intensely studied since 1980s owing to the progress in the laser induced fluorescence spectroscopy. The early works were reviewed by Driscoll, et al.[3] Especially, noble metal catalysts were studied in detail, and the reaction kinetics over Pt[4−6] and Rh[7] were quantitatively explained by the model calculations incorporating series of reactions among the neutral species. However, only a little research can be found on the oxide catalysts, lanthanide oxides by Lunsford's group[8,9] and alkaline earth oxides by ours.[10] In contrast to the noble metal catalysts, ionic species were considered to play important roles over these oxides. Although these oxides had high catalytic activity on the OH production in the reaction of H_2O and O_2, the OH concentration was controlled by the gas-phase thermodynamic equilibrium.

On the other hand, little research can be found on the OH production in the reactions of solid materials. Reck's group investigated the OH production in the laser ablation of alkaline earth hydroxides and sucrose; however, their research purpose is to derive energetic information in the ablation process.[11,12] Some of the basic hydroxides are stable at room temperature but become unstable at higher temperatures resulting in the decomposition into oxides and H_2O. If they are heated in a shorter period than the time constant of the dehydration, the OH production exceeding gas-phase thermodynamic equilibrium is expected under the partial equilibrium among the reactants and products, which is analogous to the OH production in the reaction of H_2 and O_2.[10]

In this work, the gas-phase hydroxyl radical emission in the thermal decomposition of lithium hydroxide was investigated by the temperature programmed reaction (TPR) experiments. OH was quantitatively measured by LIF and thermodynamically analyzed coupled with the measurement of other gaseous species by Q-MS. From the effect of parameters such as the amount of hydroxide, heating rates and carrier composition, the reaction mechanisms of the OH production are discussed. Moreover, the cyclic production of OH from water and oxygen is proposed in the series of the reactions of lithium compounds combined with the temperature control.

Experimental Section

The experimental system was mainly composed of a vacuum chamber, an LIF system and a Q-MS system as shown in Figure 1. Thermal decomposition of LiOH was performed in a flow tube reactor (Figure 2) settled in the vacuum chamber. It was composed of two quartz glass tubes and a ceramic heater covered with three alumina tubes. LiOH was supported on the middle alumina tube, where a K-type thermocouple was put and covered with alumina paste. After LiOH was supported and pretreated in line with the procedures shown in Table 1, TPR experiments were carried out at heating rates of 0.31−5.0 K/s under carrier gas flow (typically 2.0 Torr) with a residence time of about 70 ms over the middle alumina tube. The produced OH was measured about 2 mm above the support by OH-LIF and other stable gaseous products in the downstream of the carrier gas were measured by Q-MS.

Quantitative Measurement of OH by LIF. OH was quantitatively measured by the LIF method, which was explained in detail in our previous paper.[10] We selected the $A^2\Sigma^+(\nu' = 1) \leftarrow X^2\Pi(\nu = 0)\ Q_1(4)$ transition at 282.44 nm for the excitation of OH and the $A^2\Sigma^+(\nu' = 1) \rightarrow X^2\Pi(\nu'' = 1)$ transition around 314 nm for the observation of OH florescence. Although the collisional quenching rates, including both electronic and vibrational, were supposed to be constant in the previous paper,[10] the effect of temperature on the quenching rates should be discussed since OH was observed in a wider temperature range (900−1300 K) in this work. The quenching rate constant can be expressed as follows

* Corresponding author. Tel.: +81-3-5802-8996. (Fax: +81-3-5802-2997. E-mail: snoda@env-lab.t.u-tokyo.ac.jp.

10.1021/jp984238+ CCC: $18.00
Published on Web 02/27/1999

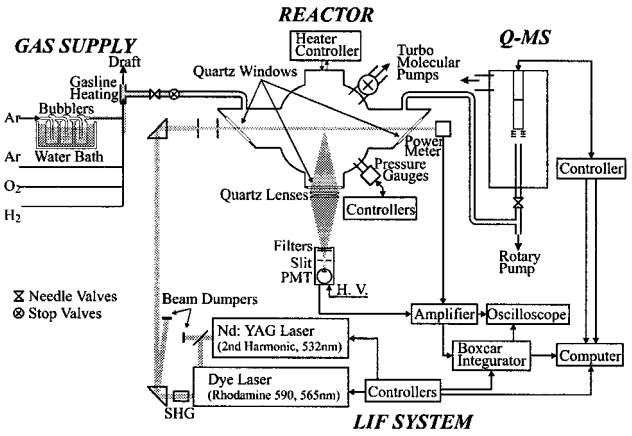

Figure 1. Schematic diagram of the experimental system.

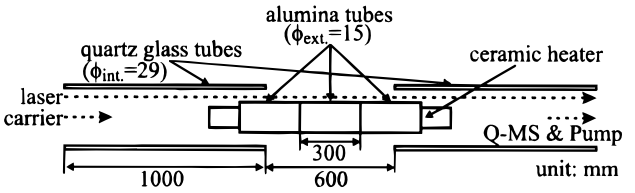

Figure 2. Schematic diagram of the cross section of the flow tube reactor.

TABLE 1: Procedures for the Pretreatment of LiOH

time [min]	procedure
0∼	paint 0.5 mL of $LiOH_{aq}$ on the alumina tube and dry it at 350−400 K.
3∼	evacuate the reactor by rotary pump
4∼	evacuate the reactor by turbo molecular pomp and start heating up
7∼	keep the reactor at specific temperature (typically at 750 K)
17∼	stop evacuation and start cooling down under carrier gas flow

TABLE 2: Quenching Rate Constants for OH (Unit: cm^3 $molecules^{-1}$ s^{-1})

collider	quenching rate constant
H_2O	$1.8 \times 10^{-11}\ T[K]^{0.5}$
H_2	$1.5 \times 10^{-11}\ T[K]^{0.5}$
O_2	$4.6 \times 10^{-12}\ T[K]^{0.5}$
Ar	$1.5 \times 10^{-13}\ T[K]^{0.5}$

$$k_q = \sigma_q u_{col} \quad (1)$$

where k_q is the quenching rate constant, σ_q is the cross section of the collisional quenching, and u_{col} is the average velocity of collision. Since u_{col} is proportional to the square root of temperature and σ_q is treated to be constant in the temperature range of this work, the final form is obtained:

$$k_q = CT^{0.5} \quad (2)$$

where C is a proportional coefficient and T is temperature. The quenching rate constants shown in Table 2 were used, which were obtained from the measurement of LIF lifetime in line with the procedures explained in our previous paper.[10]

Results and Discussion

The OH Emission in the Thermal Decomposition of LiOH. Figure 3 shows the LIF signals with increasing temperature obtained with several laser wavelengths for the OH excitation. Since the LIF signal became significant only when the wavelength was consistent with that of the OH transitions assigned by ref 13, it is clear that the LIF signal results from the OH fluorescence. In the following experiments, OH was excited by the $Q_1(4)$ rotational line.

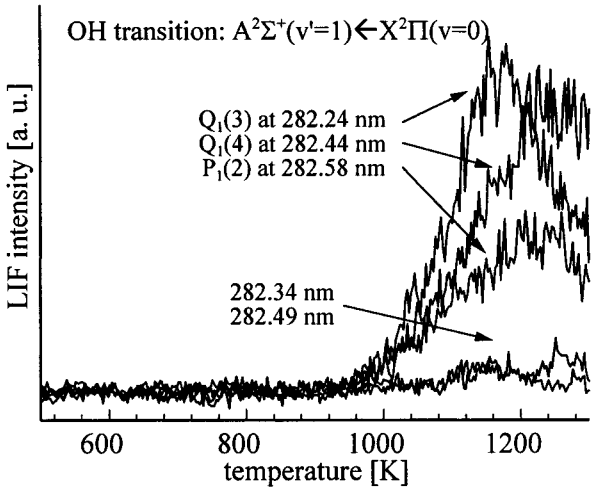

Figure 3. OH-LIF measurement with several excitation wavelengths in the TPR experiment.

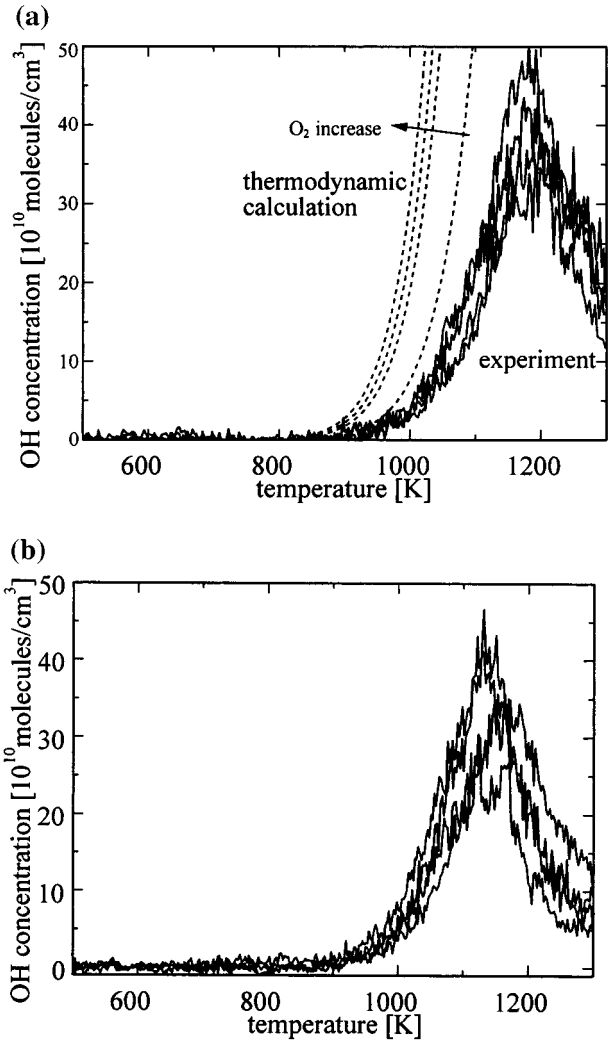

Figure 4. (a) OH emission under oxidative condition. (b) OH emission under reductive condition.

Figure 4 shows the TPR spectra of OH under the flow of the oxidative (Figure 4a) and reductive (Figure 4b) carrier gases. Since there were little effect of the carrier composition, it is clear that OH was produced neither in the gas-phase homogeneous reactions nor in the gas−solid heterogeneous catalytic

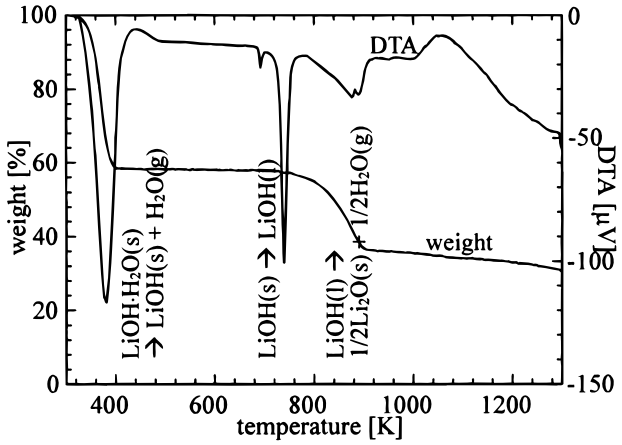

Figure 5. DG-DTA spectra of LiOH powder.

reactions. The broken curves in Figure 4a show the result of thermodynamic calculation which are discussed in the latter section. The reproducibility of the curve was good in all the experiments when the temperature was lower than that of the OH production peak, while it was not so good at higher temperatures probably due to some difference in the temperature distribution among the different alumina tubes during heating, since several alumina tubes were used in the series of the experiments.

From the results stated above, we conclude that OH was emitted in the thermal decomposition of LiOH or some other lithium compounds produced from LiOH.

Major Changes in Lithium Compounds during the Thermal Decomposition of LiOH. To understand the major changes in lithium compounds during the thermal decomposition of LiOH, thermogravimetry and differential thermal analysis (TG-DTA) of LiOH powder was carried out at a heating rate of 0.33 K/s under He carrier gas flow of atmospheric pressure. The spectra are shown in Figure 5. The first change was observed at around 380 K with an endothermic peak and a weight decrease, attributed to the dehydration of the crystal water of $LiOH{\cdot}H_2O(s)$ to form LiOH(s). The second one was observed at around 740 K with a sharp endothermic peak but without any weight change, attributed to the melting of LiOH(s) to form LiOH(l). The third one was observed at 750−900 K with an endothermic peak and a weight decrease, attributed to the dehydration reaction of LiOH(l) to form $Li_2O(s)$. After the third change, the weight kept decreasing slowly with an endothermic signal, showing the vaporization of $Li_2O(s)$ which can easily take place.[14]

To make clear the source of OH, LiOH samples evacuated at different temperatures were examined in the TPR experiment. Figure 6a shows the H_2O mole fraction in the output of the carrier gas. The samples were pretreated in line with the procedures shown in Table 1 except the temperature for evacuation. In the first sample evacuated at 400 K, where the dehydration of the crystal water of $LiOH{\cdot}H_2O$ took place, a large amount of H_2O was emitted above 700 K. In the second sample evacuated at 750 K, where the dehydration of LiOH took place, the H_2O emission decreased. In the third sample evacuated at 1050 K, no obvious change in the H_2O concentration appeared. The H_2O emission above 700 K is attributed to the dehydration of LiOH(l), which appeared at a higher temperature in the TG-DTA spectra of LiOH powder in Figure 5, due to the difference in the pressure of the carrier gas. Figure 6b shows the OH concentration measured simultaneously with the H_2O measurement. Since the OH emission was observed in

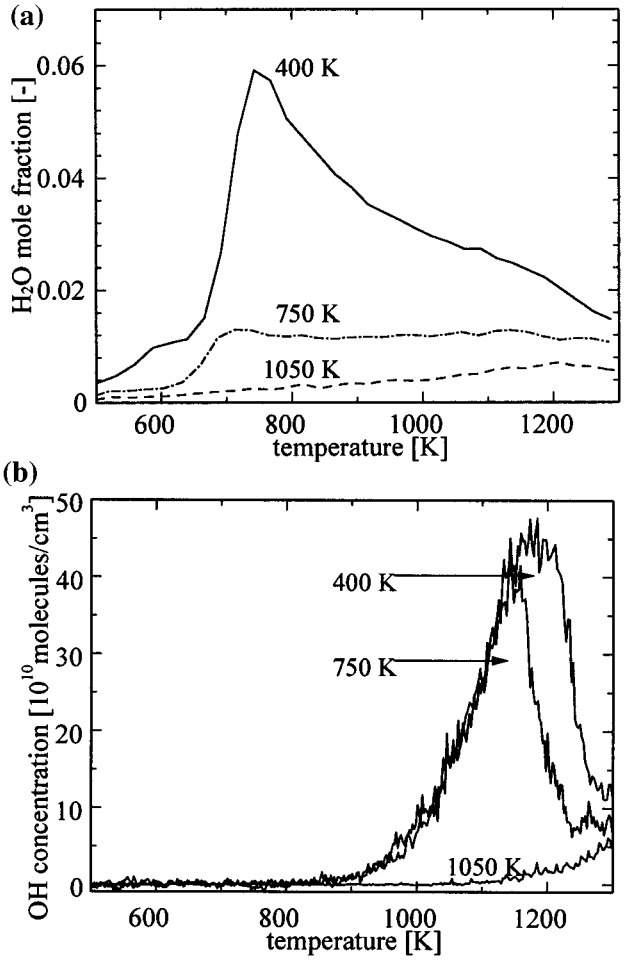

Figure 6. (a) Effect of the temperature for the sample evacuation on the H_2O production. (b) Effect of the temperature for the sample evacuation on the OH emission.

the two samples evacuated at 400 K and at 750 K, respectively, it is clear that the OH source is not the crystal water of $LiOH{\cdot}H_2O$. The much smaller difference in the OH concentration in the two samples than in the H_2O concentration shows that the OH source is not the bulk LiOH, either. These results imply that the OH source is either the surface hydroxyl group or the residual LiOH in the shape of $(Li_2O)_m(LiOH)_n$. In most of the other experimental runs, LiOH samples were evacuated at 750 K prior to the TPR experiments to suppress the heterogeneous catalytic production of OH from gas-phase H_2O.

Lithium oxides (Li_2O, Li_2O_2) and lithium hydroxide (LiOH) are the well-studied materials since lithium is expected as a breeding material of tritium in the fusion reactor blanket system. Tanaka, et al. studied the surface OH groups by FTIR.[15] They reported that the surface OH group disappeared under the He carrier gas flow at 673 K after 20 h, which was much longer than the time required in our TPR experiments (about 5 min). Tetenbaum et al. studied the solubility of LiOH in solid Li_2O under the thermodynamic equilibrium conditions.[16] From their work, it proves that LiOH exists in Li_2O with a mole fraction of about $10^{-4}-10^{-5}$ in the temperature range of 900−1300 K with 0.02 Torr of H_2O vapor, which are the typical values of our experimental conditions, even under the equilibrium conditions. From the information above, each of the surface OH group and the residual LiOH in Li_2O is still supposed to be the OH source.

Two Possible Origins of OH, the Surface OH Groups and the Residual LiOH in Li_2O. To examine whether OH originates

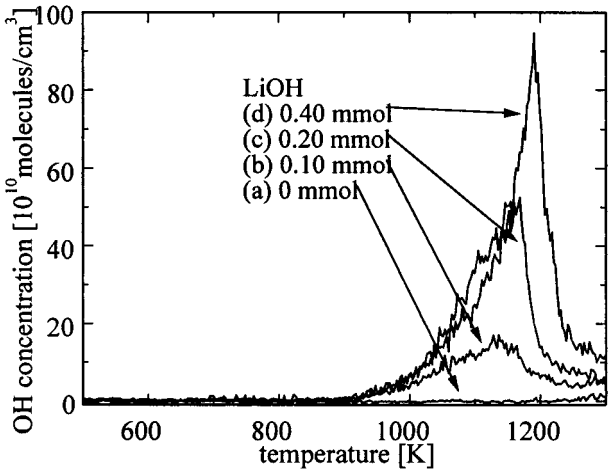

Figure 7. Effect of the amount of LiOH on OH emission.

TABLE 3: Ratio in Moles of OH to LiOH with Different Amounts of LiOH

LiOH [mmol]	OH/LiOH
0.10	4.1×10^{-5}
0.20	4.4×10^{-5}
0.40	3.7×10^{-5}

from the surface or from the bulk of lithium compounds, the effect of the amount of LiOH on the OH emission was investigated. In this experiment, we changed the amount of LiOH samples by changing the concentration of the aqueous solution of LiOH (0−0.80 M) with a constant volume of the solution (0.50 mL). Figure 7 clearly shows that the OH emission became more conspicuous as the amount of LiOH samples increased. The amount of OH can be calculated in the following equation:

$$n_{OH} = \int C_{OH} F_{carrier} dt \tag{3}$$

where n_{OH} is the amount of OH, C_{OH} is the concentration of OH, and $F_{carrier}$ is the flow rate of the carrier gas. The results were proportional to the amount of LiOH samples and the ratios in moles was almost constant within the experimental error as shown in Table 3. As for the OH concentration, it increased when the amount of LiOH increased from (b) 0.10 mmol to (c) 0.20 mmol. However, when the amount increased from (c) 0.20 mmol to (d) 0.40 mmol, the OH concentration did not change at lower temperatures than those of the peaks, and the OH emission could be observed at higher temperatures.

At first, we try to explain these results by assuming that the OH source is the surface OH groups. Typically, LiOH (0.2 mmol) was supported on the alumina surface (1.4×10^{-3} m^2) to form a Li_2O film of 1.1 μm mean thickness. To meet the amount of the OH emission, about 1×10^{-8} mol, there should be more than one OH group on the Li_2O surface of 2×10^{-19} m^2 when the surface is assumed to be flat. It seems to be possible to satisfy this quantitative requirement. If the surface area of Li_2O increases as the amount of reactant increases, both of the OH emission rate and the amount of OH should increase. This conjecture agrees with the differences observed between the experimental results (b) and (c), but does not agree with those between (c) and (d). If the surface area of Li_2O does not increase, neither of the OH emission rate nor the amount of OH should change. This conjecture does not agree with the differences observed between in (c) and (d), either. Some conflict appears between the characteristics of the OH production obtained experimentally and those predicted on the basis of the assumption at the beginning of this paragraph.

Next, we try to explain the results observed in Figure 7 by assuming that the OH source is the residual LiOH in Li_2O. Ratios in moles of the emitted OH to the supported LiOH were about 5×10^{-5} to 1 in our experiments, which is almost the same as the equilibrium solubility of LiOH in Li_2O as stated in the previous subsection. The mole fraction of the residual LiOH in Li_2O should be larger than the equilibrium solubility due to the rapid heating in our experiments so that the quantitative requirement proves to be satisfied. Qualitatively, it is supposed that the OH emission rate is determined by the surface area of the reactant, namely, the LiOH/Li_2O solid solution, and that the amount of OH is determined by the volume of the reactant. If the surface area of the reactant increases as the amount of the reactant increases, both of the OH emission rate and the amount of OH should increase. This conjecture agrees with the differences observed between the results (b) and (c), where the amounts of the reactant were relatively small. If the surface area does not increase as the amount of reactant increases, the OH emission rate should not change but the amount of OH should increase with the increase of the period of the OH emission. This conjecture agrees with the differences observed between the results (c) and (d), where the amounts of the reactant were relatively large. The experimental results can be explained without any conflict by the latter assumption.

From the discussion above, the residual LiOH in Li_2O is more probable to be the origin of OH than the surface OH groups on Li_2O.

Kinetic Observations. Figure 8a shows the effect of the heating rate on the OH emission. It is clear that the peak in the OH concentration became larger and appeared at higher temperatures as the heating rate increased, while the curves agreed well with each other at lower temperatures than that of the peak at any heating rates. The amounts of OH calculated by the eq 3 did not change so much (Table 4). These characteristics are also observed in the OH emission from different amounts of LiOH, which has already been explained in the previous subsection (Figure 7 and Table 3). From these two experiments, it proves that the OH production rate is decided only by temperature at lower temperatures than that of the OH emission peak, when enough amount of the reactant remains. The following equations can be formed on the reaction rate:

$$R_{OH} = k_{OH} f(C_{react}) \tag{4}$$

where R_{OH} is the production rate of OH per surface area, k_{OH} is the rate constant, $f(C_{react})$ is some function of the concentration of the reactant, probably being equal to C_{react}. There is the following relation between the reaction rate and the OH concentration:

$$C_{OH} = \frac{AR_{OH}}{F_{carrier}} \tag{5}$$

where A is the surface area of the reactant. Since $f(C_{react})$, A and $F_{carrier}$ are constant at lower temperatures than those of the OH emission peak where the conversion of the reactant is small, C_{OH} proves to be proportional to the rate constant (k_{OH}). Figure 8b shows the Arrhenius plots of a part of the experimental results shown in Figure 8a, where the OH concentration is used in place of the rate constant. It is clear that the OH production rate can be plotted on one line with an apparent activation energy of 140 kJ/mol at the lower temperatures than that of the OH emission peak and thus the OH emission rate is determined only

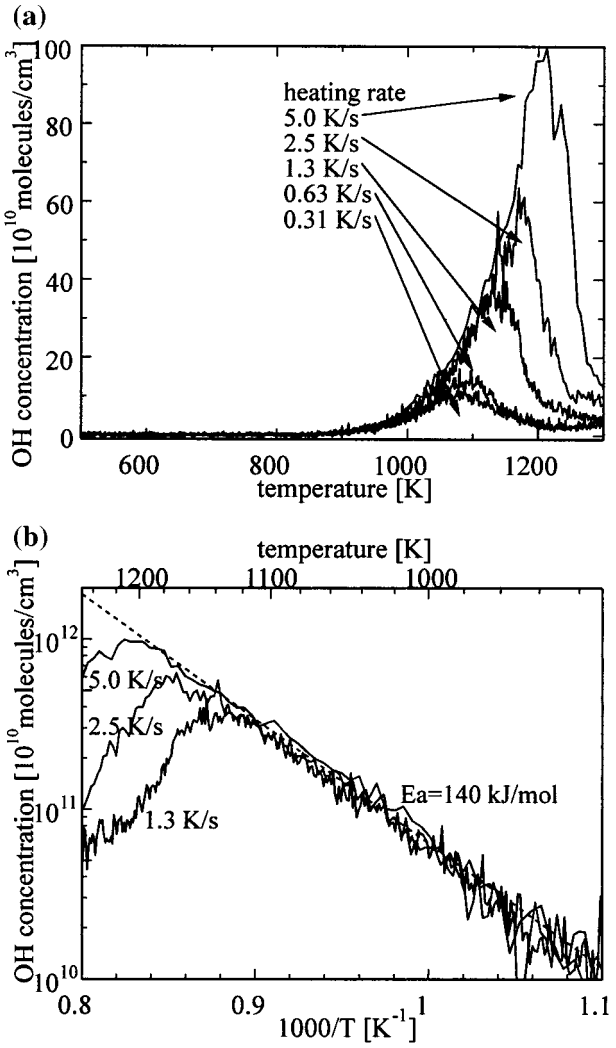

Figure 8. (a) Effect of heating rate on OH emission. (b) Arrhenius plots of the OH concentration with different heating rates.

TABLE 4: Ratio in Moles of OH to LiOH at Different Heating Rate

heating rate [K/s]	OH/LiOH
0.31	11×10^{-5}
0.63	6.4×10^{-5}
1.3	7.6×10^{-5}
2.5	5.9×10^{-5}
5.0	5.0×10^{-5}

by temperature. This fact agrees with both of the two conjectures in the previous subsection based on the two different assumptions on the origin of OH.

Thermodynamic Analysis. The solid line in Figure 9 shows a typical TPR spectrum of OH. From the Q-MS measurement, the mole fraction of H_2O and O_2 in the carrier gas proved to be less than 1% and 0.1%, respectively. Using these values, we estimated the maximum OH concentration under the thermodynamic equilibrium condition (the broken line) by the calculation based on the work by Gordon and McBride.[17] From these two lines, it is clear that the concentration of OH emitted from LiOH was much larger than the thermodynamic equilibrium value. If the LiOH sample is heated quasistatically, the concentration of gas-phase OH should be the same as the thermodynamic equilibrium value. The OH concentration exceeding the equilibrium value suggests that the dehydration of LiOH, which is the main reaction controlling the equilibrium, did not follow the temperature increase of the reactant.

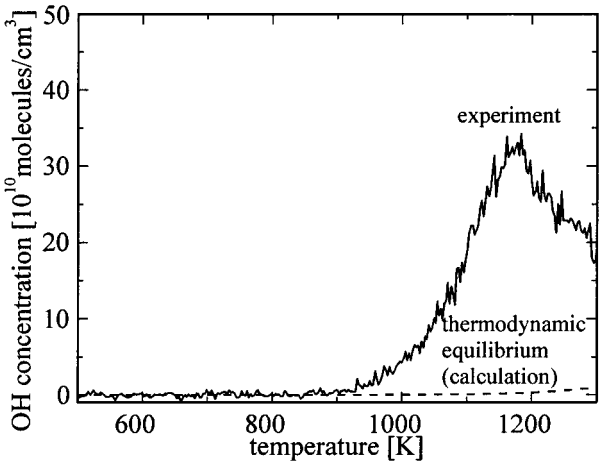

Figure 9. Comparison of the typical temperature profile of the OH concentration in the TPR experiment and that obtained in the thermodynamic equilibrium calculation.

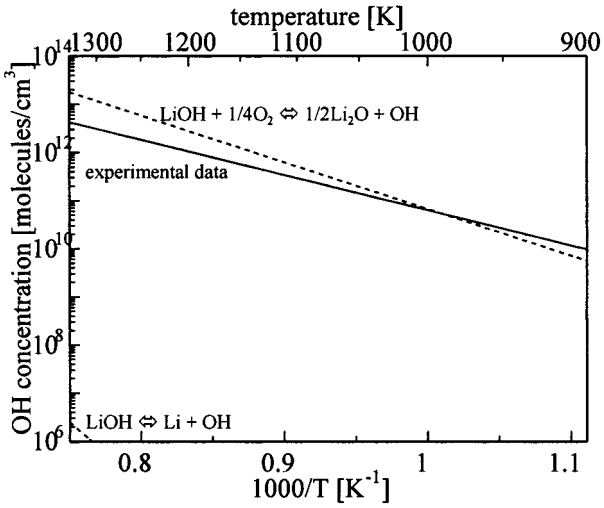

Figure 10. Arrhenius plots of the OH concentration obtained in the TPR experiment (a solid line) and partial equilibrium concentrations calculated for the two reactions (broken lines).

Since one of the possible sources of OH is the residual LiOH in the $LiOH/Li_2O$ as stated above, the following reactions are listed up which may control the partial equilibrium of the OH production:

$$LiOH \rightarrow Li + OH \quad (6)$$

$$LiOH + {}^1/_4O_2 \rightarrow {}^1/_2Li_2O + OH \quad (7)$$

Using the thermodynamic data of the pure materials in the JANAF tables,[18] we calculated the partial equilibrium concentration of OH in each reaction. Figure 10 shows the Arrhenius plots of the OH concentration obtained in the TPR experiment (a solid line) and those in thermodynamic calculations (broken lines). It is clear that the contribution of the reaction 6 is negligible. For reaction 7, the equilibrium concentration was calculated with the O_2 partial pressure of 2 mTorr, which is the typical value in the experiment. From this figure, it proves that reaction 7 can control the partial equilibrium. In this reaction, the partial equilibrium concentration should be effected by the partial pressure of O_2. Figure 4a shows the results obtained in the experiments and those obtained from the calculation with the different O_2 partial pressures. The concentration in both results proves to be in the same range, while the effect of the

O_2 partial pressure is observed only in the thermodynamic calculations. If the reaction 7 is composed of the following two elementary reactions:

$$\mathrm{LiOH} \rightarrow \mathrm{Li} + \mathrm{OH} \tag{6}$$

$$\mathrm{Li} + {}^1/_4\mathrm{O}_2 \rightarrow {}^1/_2\mathrm{Li}_2\mathrm{O} \tag{8}$$

and the reaction 6 is the rate determining step under the experimental conditions, the effect of O_2 partial pressure should not appear in the OH concentration. Since the discussion above is based on the thermodynamics only of the pure materials, there may be some other reactions which can explain the experimental results if we consider the thermodynamics of the defective materials such as Li_2O_{1-x} ($0 < x \ll 1$).

From these results, we conclude that the OH emission exceeding the equilibrium was realized by the partial equilibrium in some reactions such as reaction 7.

Possibility of the Cyclic Production of OH by the Series of the Reactions of Lithium Compounds. Since LiOH is easily formed under the existence of H_2O and O_2 near ambient temperature, we can design reaction cycles for the OH production. If the OH production is controlled by the reaction 7, the following cycle is possible:

The OH production at high temperatures.

$$\mathrm{LiOH} + {}^1/_4\mathrm{O}_2 \rightarrow {}^1/_2\mathrm{Li}_2\mathrm{O} + \mathrm{OH} \tag{7}$$

Regeneration of LiOH at low temperatures under exposure to H_2O.

$$ {}^1/_2\mathrm{Li}_2\mathrm{O} + {}^1/_2\mathrm{H}_2\mathrm{O} \rightarrow \mathrm{LiOH} \tag{9}$$

The total reaction composed of these two reactions becomes as follows:

$$ {}^1/_2\mathrm{H}_2\mathrm{O} + {}^1/_4\mathrm{O}_2 \rightarrow \mathrm{OH} \tag{10}$$

which is the same as that in the catalytic production of OH from H_2O and O_2.[8−10]

Conclusions

Gas-phase OH radicals were produced in the thermal decomposition of LiOH with a concentration largely exceeding the thermodynamic equilibrium. The origin of OH was supposed to be either the surface OH groups on Li_2O or the residual LiOH in the $LiOH/Li_2O$ solid solution. OH production exceeding the thermodynamic equilibrium was explained by means of the partial equilibrium in the reaction: $\mathrm{LiOH} + {}^1/_4\mathrm{O}_2 \leftrightarrow {}^1/_2\mathrm{Li}_2\mathrm{O} + \mathrm{OH}$. It may be possible to produce OH from H_2O and O_2 in some cyclic reactions of lithium compounds with the temperature control.

Acknowledgment. This work has been supported by CREST (Core Research for Evolutional Science and Technology) of Japan Science and Technology Corporation (JST).

References and Notes

(1) Seinfeld, J. H. *Atmospheric Chemistry and Physics of Air Pollution*; Wiley-Interscience: New York, 1986.
(2) Pfefferle, L. D.; Griffin, T. A.; Winter, M.; Crosley, D. R.; Dyer, M. J. *Combust. Flame* **1989**, *76*, 325.
(3) Driscoll, D. J.; Campbell, K. D.; Lunsford, J. H. *Adv. Catal.* **1987**, *35*, 139.
(4) Hsu, D. S. Y.; Hoffbauer, M. A.; Lin, M. C. *Surf. Sci.* **1987**, *184*, 25.
(5) Williams, W. R.; Marks, C. M.; Schmidt, L. D. *J. Phys. Chem.* **1992**, *96*, 5922.
(6) Fridell, E.; Rosén, A.; Kasemo, B. *Langmuir* **1994**, *10*, 699.
(7) Mallen, M. P. Zum; Williams, W. R.; Schmidt, L. D. *J. Phys. Chem.* **1993**, *97*, 625.
(8) Anderson, L. C.; Xu, M.; Mooney, C. E.; Rosynek, M. P.; Lunsford, J. H. *J. Am. Chem. Soc.* **1993**, *115*, 6322.
(9) Hewett, K. B.; Anderson, L. C.; Rosynek, M. P.; Lunsford, J. H. *J. Am. Chem. Soc.* **1996**, *118*, 6992.
(10) Noda, S.; Nishioka, M.; Harano, A.; Sadakata, M. *J. Phys. Chem. B* **1998**, *102*, 3185.
(11) Deshmukh, S.; Rithe, E. W.; Reck, G. P. *J. Phys. Chem.* **1991**, *95*, 8385.
(12) Villanueva, J.; Deshmukh, S.; Reck, G. P. *J. Phys. Chem.* **1993**, *97*, 11731.
(13) Dieke, G. H.; Crosswhite, H. M. *J. Quantum. Spectrosc. Radiat. Transfer* **1962**, *2*, 97.
(14) Kudo, H.; Wu, C. H.; Ihle, H. R. *J. Nucl. Mater.* **1978**, *78*, 380.
(15) Tanaka, S.; Taniguchi, M. Nakatani, M.; Yamaki, D.; Yamawaki, M. *J. Nucl. Mater.* **1995**, *218*, 335.
(16) Tetenbaum, M.; Fischer, A. K.; Johnson, C. E. *Fusion Technol.* **1985**, *7*, 53.
(17) Gordon, S.; McBride, B. J. Report NASA SP-273; NASA: Washington, DC, 1971.
(18) Chase, Jr., M. W.; Davies, C. A.; Downey, Jr., J. R.; Frurip, D. J.; McDonald, R. A.; Syverud, A. N. *J. Phys. Chem. Ref. Data, Suppl.* **1985**, *14* (1).